Nanoscale

Accepted Manuscript

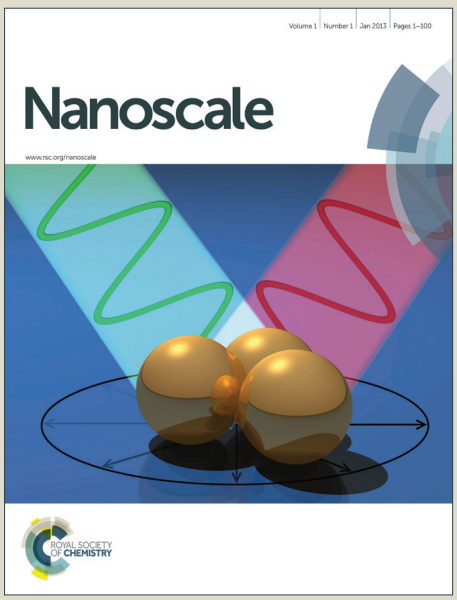

ROYAL SOCIETY OF CHEMISTRY

www.rsc.org/nanoscale

Cite this: DOI: 10.1039/c0xx00000x

www.rsc.org/xxxxxx

ARTICLE TYPE

Nanocellulose Coupled Flexible Polypyrrole@Graphene Oxide Composite Paper Electrodes with High Volumetric Capacitance

Zhaohui Wang,[a]* Petter Tammela,[b] Maria Strømme,[b] Leif Nyholm[a]

Received (in XXX, XXX) Xth XXXXXXXXX 20XX, Accepted Xth XXXXXXXXX 20XX

DOI: 10.1039/b000000x

A robust and compact freestanding conducting polymer-based electrode material based on nanocellulose coupled Polypyrrole@Graphene oxide paper is straightforwardly prepared *via* in-situ polymerization for use in high-performance paper-based charge storage devices, exhibiting stable cycling over 16 000 cycles at 5 A g^{-1} as well as the largest specific volumetric capacitance (198 F cm^{-3}) so far reported for flexible polymer-based electrodes.

The increasing energy consumption and the demands for inexpensive portable electronic have turned the attention of researchers toward sustainable and smart power sources. As a result of this there is a strong requirement for the development of flexible and lightweight electrode materials for the next generation of energy storage devices.[1-6] In this process, electroactive conducting polymers (ECPs), such as polypyrrole (PPy) and polyaniline (PANI) are highly promising since it has been shown that these can be used to manufacture polymer-based supercapacitors owing to their inherent high capacity, flexibility and versatility, as well as lightweight and low-cost.[1, 7-11] However, their limited post-synthesis processability due to their poor solubility, infusibility, and mechanical brittleness[1] is generally considered a major drawback regarding the applicability of ECPs in flexible supercapacitors. Recently, significant efforts have therefore been made to fabricate ECPs-based flexible electrodes employing various types of carbon materials (e.g., graphene, and carbon nanotubes (CNTs)) which have emerged as an effective solution to achieve the above goals.[12-23] Reports on flexible PPy or PANI-based electrodes which can be directly used as freestanding electrodes (i.e. without additional substrates), are nevertheless still sparse. In addition, a large amount of CNTs or graphene (corresponding to at least 30 - 40 wt.%) were generally employed which complicates the development of low-cost and environmentally friendly energy-storage system for high-power applications. The quest for sustainable and inexpensive freestanding flexible ECPs-based electrodes for sustainable energy storage devices therefore remains a challenge.

Cellulose, which is one of the most abundant organic materials on earth and the major component in paper, has recently been widely used in conjunction with electroactive materials to fabricate flexible energy storage devices with high mechanical strength and flexibility.[24-26] Cellulose combined with graphene have thus demonstrated versatile feasibility for the development of flexible electronics,[27-29] while paper electrodes made from nanocellulose and PPy have been shown to be promising for low-cost and sustainable charge storage devices.[30-33] The possibilities of armouring the nanocellulose fibers with graphene and ECPs to obtain materials with high capacitances, low cost, mechanical flexibility and robustness, as well as the subsequent moulding of the electrode composites into soft paper sheets of desired shapes, are therefore highly appealing. Such an ECP-cellulose-graphene hybrid nanocomposite has, however, to the best of our knowledge not yet been presented.

When used as electrodes for charge storage devices, gravimetric capacitances of about 250 F g^{-1} have been reported for cellulose/ECPs[30, 32] and cellulose/graphene composites[27]. Since the volumetric capacitances are significantly less competitive due to the relatively low density of the composites it is, however, difficult to develop compact storage devices based on these materials.[34] Although flexible yet dense ECPs-based electrodes with high volumetric capacitances and little environment impact are very promising in contemporary electrochemical energy storage devices, such electrodes and devices have so far proved very challenging to produce.[34]

Herein, we demonstrate a novel straightforward approach for the preparation of flexible and compact PPy@Nanocellulose@Graphene oxide (PNG) paper electrodes containing only 5.8 wt.% graphene oxide as a reinforcing and structural directing additive, employing a facile in-situ chemical polymerization method. The obtained self-standing, binder-free, dense and flexible PNG paper-based material, which exhibits the largest volumetric capacitance of 198 F cm^{-3} reported so far for flexible ECPs-based electrodes, have been utilized in symmetric charge storage devices demonstrating stable cycling over 16 000 cycles at a current density of 5 A g^{-1}.

The new and versatile approach has several advantages with respect to current state-of-the art methods since i) strong bonding between the nanocellulose and graphene oxide (GO) as well as the PPy coating, which guarantees the integrity of the electrode and allows the preparation of compact electrodes; ii) nanocellulose is attached to two-dimensional (2D) PPy@graphene oxide where the latter not only acts as a reinforcement to improve the mechanical properties but also provides a 3D structure of interconnected pores available as ionic transport pathways;[35] iii) the PNG paper in which the high conductivity and capacitance of PPy is combined with the

flexibility and high surface area of GO, holds great promise to overcome the low mechanical strength and density problems associated with PPy@nanocellulose papers[31, 32] and PPy@graphene nanocomposites, [36, 37] while simultaneously outperforming the low capacitance CNTs/cellulose[38] and graphene-nanocellulose papers[39] which mainly store energy within the electrical double-layer; iv) new possibilities for up-scaling based on traditional cost-effective paper-making processes are available. It is therefore reasonable to assume that a flexible polymer electrode composed of nanocellulose, GO and PPy, exhibiting a high volumetric capacitance and good cycling stability, may significantly facilitate the development of compact, low-cost and environmentally friendly paper-based charge storage devices.

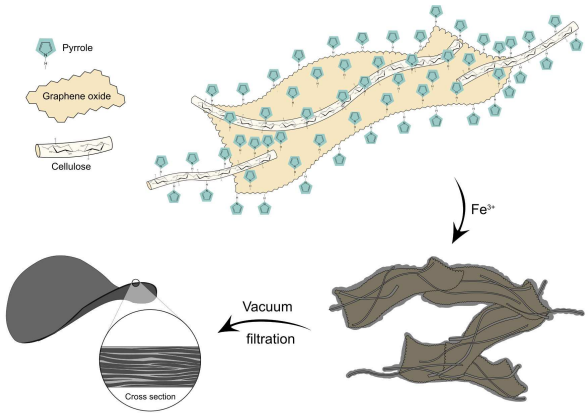

Figure. 1 Schematic illustrations depicting the preparation and structure of the PNG paper electrodes.

As shown in the schematic illustration in **Figure 1,** the present strategy relies on the unique structure of the nanocellulose fibers containing abundant functional groups which give rise to strong inter- and intramolecular hydrogen bonds and thus provide strong bonds between the components of the composite. It should also be pointed out that nanocellulose can serve as an aqueous dispersion agent to prevent restacking between graphene layers.[28, 40] By introducing an oxidation agent (e.g. Fe(III) nitrate), a PPy layer can straightforwardly be polymerized both on the nanocellulose attached to the GO sheets and the GO itself. This approach, which provides a porous composite with a large electrolyte-accessible surface area, also allows flexible and compact PNG paper-like composite electrodes to be readily obtained by solution casting after the polymerization step (see the Experimental section and **Figure 1**).

Fourier-transform infrared (FTIR) spectroscopy results for the PNG composite show well-defined peaks at 3352, 1113, 1057 and 1033 cm^{-1} in **Figure 2a**, which can be ascribed to the -OH glucose ring stretch and C-OH stretching vibrations of cellulose,[41] respectively. Compared to the FTIR spectrum for the nanocellulose fibers, several characteristic PPy peaks can also be found in the PNG paper electrode spectrum. The peaks at 1542, 1307, 1169, and 1029 cm^{-1} are thus assigned to the vibrations of -C=C, -C-H, -C-N-C, and -N-H,[42] respectively, which demonstrates that PPy was successfully incorporated into the flexible paper electrode material. The presence of a PPy coating layer on the cellulose and GO is further supported by X-ray diffraction (XRD) data (see **Figure S1, in the supporting information (SI)**). The FTIR data further indicate that some characteristic nanocellulose peaks due to C=O and C-OH were absent for the PNG composite and that the GO peaks were absent for the PNG composite. This indicates that a layer of PPy was present on the nanocellulose and the GO. The absence of the GO peaks can also be explained by the low mass percentage of GO (5.8 wt.%) within the composite.

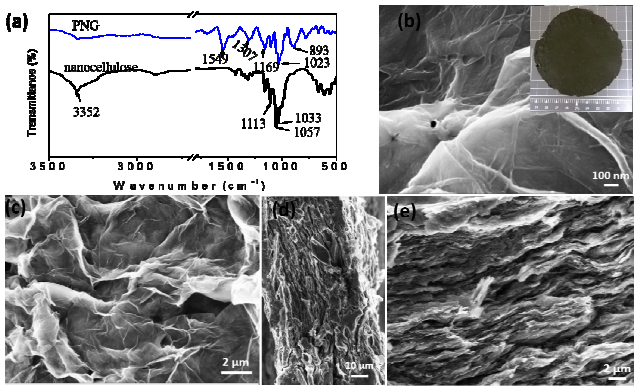

Figure 2 (a) FTIR spectra for nanocellulose and a PNG paper composite, respectively. (b) Digital image of a PNG paper composite. (c) and (d) SEM images of a PNG paper composite at different magnifications. (e) and (f) Cross-section SEM images of a PNG paper composite at different magnifications.

The insert in **Figure 2b** shows digital images of the freestanding PNG paper electrode with a dark-grey colour. The paper-sheet had a diameter of 9 cm which demonstrates the possibilities to straightforwardly produce relatively large flexible electrodes. The nanostructure of the PNG paper sheets were first studied by scanning electron microscopy (SEM). As is shown in **Figure 2b** and **2c**, the PNG composites were composed of a large quantity of wrinkled and crumpled nanosheets with rough surfaces interconnected to form a free-standing integrated film. The PPy/GO composites (i.e. composites lacking nanocellulose) prepared under identical conditions could, on the other hand, only be obtained as powders (see **Figure S2**, **Figure S3d**) featuring individual curved nanosheets with smoother surfaces (**Figure S3a-3c**). These results clearly demonstrate that PPy/GO cross-links are needed for the attainment of free-standing and flexible PNG composite electrodes. It should also be mentioned that the nanocellulose mass fraction has an effect on the morphology of PNG electrodes. As shown in **Figure S4**, PNG composites prepared with higher nanocellulose contents (e.g. a nanocellulose : GO ratio of 10:1) show two main features: the fine fibrillar structure typical of PPy@nanocellulose composites[8, 31, 33, 43, 44] combined with the PNG wrinkled and crumpled nanosheets in which both components are intertwined and PPy@nanocellulose are embedded all over the surface of the PPy@GO nanosheets (see **Figure S4a** and **S4b**). A further increase in the nanocellulose : GO ratio to 20:1 resulted in a higher content of PPy@nanocellulose fibers as can be expected based on our previous studies,[8, 31] although nanocellulose-PPy-GO features still can be observed (see **Figure S4c** and **S4d**).

Based on these results, which demonstrate the shape and structure directing effect of nanocellulose during the formation of PNG paper electrodes, it is reasonable to assume that the PNG composites should be able to provide both good mechanical strength and high electrical conductivity. **Figure 2d** further shows a cross-section SEM image of the freestanding PNG paper sheet with thickness of ~ 55 µm. The PNG paper electrodes exhibited a compact layer-by-layer stacking structure (see **Figure 2e)** as a result of the directional flow induced by the vacuum filtration step, in good agreement with previous results for reduced graphene oxide (rGO)/cellulose composite papers.[29] In addition, the PNG paper had a density of around 1.25 g cm^{-3} which, incidentally, is a factor of two higher than for the carbon electrodes generally used in high volumetric capacitance energy storage devices.[45] The Brunauer - Emmett - Teller (BET) specific surface area of the PNG paper electrode was 28.8 m^2 g^{-1} and the results also indicated that the material was mesoporous **(**see **Figure S5)**. The latter suggests that the dense packing of the PNG paper still allows sufficient contact between the electrolyte and the composite to allow efficient and rapid charge storage.

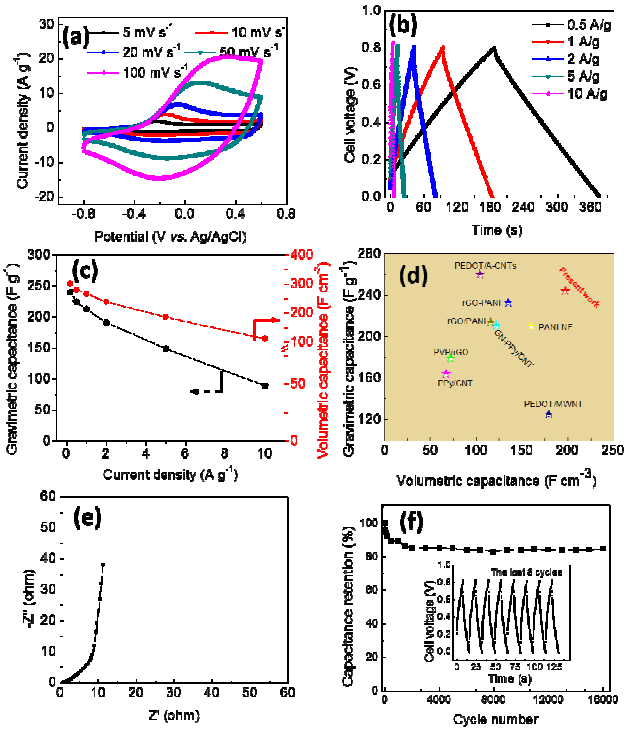

Figure 3 Electrochemical characterization of PNG paper composite electrodes. (a) Cyclic voltammograms recorded in a 2.0 M NaCl aqueous solution using a three-electrode setup and different scan rates. (b) Galvanostatic charge/discharge curves obtained for a symmetric PNG based charge storage device. (c) Specific gravimetric and volumetric capacitances as a function of the current density. (d) Comparison of the PNG electrode specific gravimetric and volumetric capacitance with values reported for other flexible polymer electrodes, such as PVP/GO,[14] GN-PPy/CNT,[16] PPy/CNT,[16] rGO-PANI,[18] PEDOT/A-CNTs,[21] PANI-NF,[22] PEDOT/MWNT.[23] (e) Nyquist plot and (f) the long-time cycling performance at 5 A g^{-1}. The last eight charge/discharge cycles are displayed in the inset.

To evaluate the charge storage performance of the PNG paper electrodes, cyclic voltammograms (CVs) were recorded with a three-electrode setup in a 2 M NaCl aqueous solution. As is shown in **Figure 3a**, all voltammograms exhibited similar and symmetric shapes as the scan rate was increased from 5 to 100 mV s^{-1}, suggesting a well-defined PPy redox behaviour for the PNG paper electrodes. To further investigate the electrochemical behaviour of the PNG electrodes, symmetric charge storage devices (containing two identical PNG electrodes separated by a filter paper soaked with a solution of 2 M NaCl) were fabricated and subsequently subjected to galvanostatic charge/discharge experiments at different current densities in a cell voltage window between 0 and 0.8 V. As is seen in **Figure 3b**, all the charge/discharge curves exhibited nearly linear shapes and the charge and discharge curves remained practically symmetric even at a current density of 10 A g^{-1}, demonstrating a remarkable reversibility for the PNG electrodes. The small voltage drop between 0.7 and 0.8 V for the symmetric devices, which was caused by the equivalent series resistance, was significantly smaller than that seen for the PPy/GO electrode (see **Figure S6a**). This shows that the resistance of the free-standing continuous PNG electrodes was significantly smaller than those of the PPy/GO electrodes for which additives such as binder and carbon black were required in the electrode manufacturing process.

The specific gravimetric capacitance of the PNG paper electrode (obtained from the galvanostatic discharge curves by multiplying the device capacitance by a factor of four) was 244 F g^{-1} at a current density of 0.2 A g^{-1}. The latter is comparable to or even better than previously reported values for PPy/rGO[46, 47] and PPy/CNT electrodes.[16, 48] Although the specific capacitance decreased with increasing current density, a capacitance of 90 F g^{-1} was still obtained for a current density of 10 A g^{-1} (**Figure 3c**). For the PPy/GO composite, a specific capacitance of 48 F g^{-1} at 5 A g^{-1} was, on the other hand, obtained (see **Figure S6b**), demonstrating that the free-standing PNG electrode yielded a higher gravimetric specific capacitance than the PPy/GO material. This clearly shows the energy storage advantage of the binder-free and self-standing PNG paper electrodes, in which the nanocellulose served to maintain the mesoporous electrode integrity yielding an efficient and fast ion transport.[35] More importantly, as the PNG electrodes exhibited remarkable volumetric capacitances (i.e. 112 F cm^{-3} at 10 A g^{-1}) owing to its highly compact structure, these electrodes are highly promising for future charge storage applications. The volumetric capacitance of the PNG electrode at 0.2 A g^{-1} was, in fact, found to be 198 F cm^{-3} (corresponding to 301 F cm^{-3} based on PPy) (see **Figure 3d, Table S1**). This is an extremely high value for a conducting polymer based electrode. Given the fact that the PNG electrodes also are strong and highly flexible (as is described below), the materials are indeed very promising for use in flexible energy storage systems.

In the Ragone plot in **Figure S7**, it is seen that the maximum volumetric energy and power densities of the PNG paper electrode (calculated as described in the electrode evaluation section) were 3.4 Wh L^{-1} and 1.1 kW L^{-1} (corresponding to 5.1 Wh kg^{-1} and 1.5 kW kg^{-1}), respectively. As the latter energy density is comparable to those for many commercial carbon/carbon capacitors (i.e. 5 ~ 8 Wh L^{-1}) working in high potential windows in organic solvents,[45] while

the power density (i.e. 1.1 kW L^{-1}) is much higher than those reported for charge storage devices comprising flexible polymer-based electrodes (0.4~1 kW L^{-1}),[14, 30, 36] it is immediately evident that these symmetric PNG devices hold great promise for paper based energy storage applications.

The PNG symmetric energy storage devices were also studied using electrochemical impedance spectroscopy (EIS). As is seen in **Figure 3e**, the equivalent series resistance was found to be approximately 0.7 Ω. The absence of a semi-circle and the presence of the line with a 45º slope in the Nyquist plots followed by a close to ideal capacitive behaviour indicate that the PPy redox reactions were diffusion controlled and that a (pseudo)capacitive response associated with finite length diffusion (i.e. a thin-layer behaviour) was seen at sufficiently low frequencies, in good agreement with previous findings.[49]

The long-time cycle performance of the symmetric devices based on the PNG paper electrode was investigated employing a current density of 5 A g^{-1} and a cell voltage window between 0.0 and 0.8 V. As is depicted in **Figure 3f**, a specific electrode capacitance loss was observed during the first 1000 cycles after which the capacitance remained almost unchanged. This initial decrease in the capacitance (which often is seen for conducting polymer-based devices[13, 22, 50]) could be related to the fact that the potential distribution between the two PNG electrodes undergo significant changes during the initial part of the cycling, a process which also involves some degradation of the positive electrode.[51] This hypothesis is supported by the fact that the initial and final cycling curves generally exhibited significantly different shapes (the insert in **Figure 3f** shows last eight charge/discharge curves for which the coulombic efficiency was very close to 100 %). After 16 000 cycles, the electrode capacitance was stable at a value corresponding to about 85% of its initial value, which is much better than those found for ECPs-based energy storage devices (see **Table S1**), demonstrating that flexible PPy-based charge storage devices are able to charge/discharge over 10000 cycles without significant additional loss of capacitance.

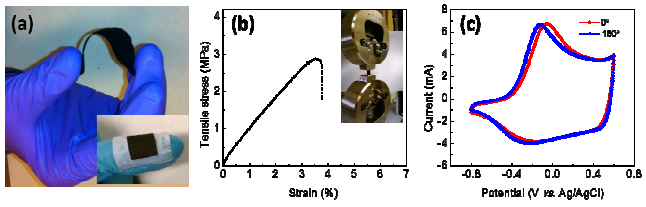

Figure 4 (a) Digital photographs of a PNG paper electrode showing its flexibility during bending (b) Stress - strain curve for a PNG paper electrode (c) Cyclic voltammograms for PNG paper electrodes recorded with two different bending angles, i.e. 0° and 180°, at a scan rate of 20 mV s^{-1}.

As has already been indicated above, it is reasonable to assume that the PNG paper could be used as a flexible electrode material. To investigate the flexibility of the material the electrodes were subjected to repetitive bending as well as experiments in which the tensile stress was measured employing stress-strain experiments. As is seen in **Figure 4a,** the freestanding PNG paper was highly flexible and could be bent repeatedly without any obvious mechanical destruction. This can be ascribed to the strong bonds between the nanocellulose and GO which result in a mechanical reinforcement of the composite by nanocellulose, as well as the inherent flexibility of both the PPy and the GO. The PNG paper electrode was not only flexible but also mechanical robust as is shown in **Figure 4b** depicting the results of a stress - strain test. A tensile strength of 2.9 MPa at a strain of 3.7% was thus obtained indicating good mechanical properties. To test the electrochemical performance of the PNG paper electrode under bending conditions, cyclic voltammetry experiments were further performed on the paper electrodes employing two different bending angles, i.e. 0° and 180° and a scan rate of 20 mV s^{-1}. As shown in **Figure 4c**, no obvious difference could be seen between the voltammograms, which suggests that the PNG paper electrodes may indeed be used in flexible-device applications. It should also be pointed out that the active mass loading (i.e. ~ 4.2 mg cm^{-2}) of the PNG electrodes was significantly higher than those (~ 1 mg cm^{-2})[13, 17, 20, 30] reported for the previously studied flexible electrodes containing conducting polymers. In addition, the PNG electrode was rather compact and had a density of about 1.25 g cm^{-3}, which is higher than for most previously presented flexible conducting polymers-based electrodes (see **Table S1**).

It is worth to point out that PNG electrodes with larger nanocellulose:GO ratios (i.e. 10:1 and 20:1) were destroyed upon bending, their electrochemical performance was shown in the **Figure S8**. It is seen that the cell capacitance decreased with decreasing nanocellulose:GO ratios. In the Nyquist plots (**Figure S8b**), it can be seen that a decreased nanocellulose:GO ratio resulted in a larger influence of diffusion most likely as a result of the attainment of a more compact composite. The latter is in good agreement with the lower cell capacitances found for the lower nanocellulose:GO ratios seen at increased current densities. These results thus indicate that the incorporation of GO into the composite gives rise to a more compact and flexible composite and that the electrochemical and mechanical properties of the composite can be tailored by varying the nanocellulose:GO ratio. Higher ratios clearly yield higher cell capacitances at high current densities but poor flexibilities.

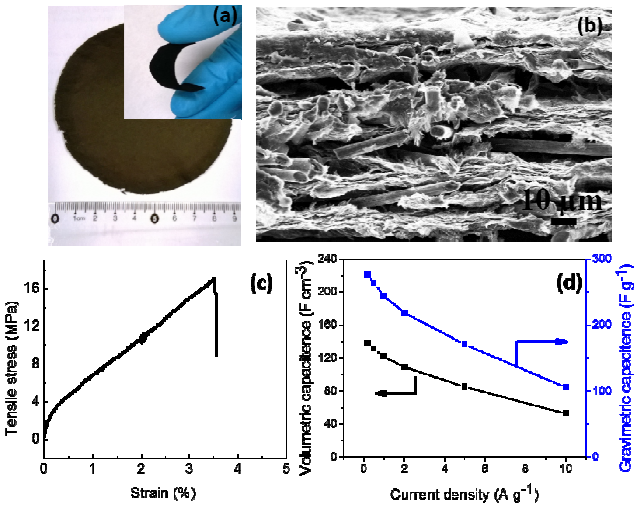

Figure 5. (a) Digital image of a CCF-PNG paper electrode. The inset shows the flexibility of the CCF-PNG composite. (b) Cross-section SEM

image for a CCF-PNG paper electrode. (c) Stress - strain curve for a CCF-PNG paper electrode. (d) Specific gravimetric and volumetric capacitances versus the current density for a CCF-PNG paper electrode.

As is demonstrated in **Figure 5**, an even stronger flexible PNG paper can be obtained by including (~ 23 wt.%) chopped carbon fibers (CCF) into the PNG composite. The CCF-reinforced PNG paper (CCF-PNG), which had the appearance of a black glossy paper, could be readily bent back and forth at different angles. From surface SEM images of the present CCF-PNG electrodes (see **Figure S9**), .no significant difference in morphology and porosity as compared to the PNG electrodes can be seen. In the CS-SEM image in **Figure 5b** it can be seen that the material exhibited an open structure in which the 7-8 µm-thick fibers randomly pierced through the layered PNG paper electrode. Thanks to the high specific tensile stiffness and ultimate tensile strength of the CCF, the CCF-PNG paper electrode displayed a tensile strength of 17.8 MPa (see **Figure 5c**) which exceeds the values for all other flexible polymer-based electrodes presented this far.[17, 18, 20, 22, 30, 52, 53] The gravimetric specific capacitance for the CCF-PNG paper electrode calculated from the galvanostatic discharge curves (see **Figure S10**) as previously described was 276 F g^{-1} at a current density of 0.2 A g^{-1}. This value is somewhat higher than the 244 F g^{-1} obtained for the PNG paper electrode. The CCF-reinforced PNG electrodes, also exhibited a slightly better capacitance at a high rate than the PNG electrode (i.e. 107 F g^{-1} as compared to 90 F g^{-1} at 10 A g^{-1}, see **Figure 5d**). One explanation for this could be the lower active mass loading (i.e. ~ 3.4 mg cm^{-2} as compared to ~ 4.2 mg cm^{-2}) for the CCF-PNG paper electrode as a lower active mass loading results in a smaller iR drop. The density of the CCF-reinforced PNG electrode (i.e. 0.8 g cm^{-3}) was, however, much smaller than that for the PNG paper which resulted in significantly lower volumetric capacitances (see **Figure 5d**). A volumetric capacitance of 138 F cm^{-3} could still be obtained for the CCF-PNG paper electrode, which is higher than the values reported for many flexible polymer-based electrodes (see **Table S1**). It is therefore evident that both the PNG and CCF-PNG approaches constitute versatile and straightforward methods for the fabrication of robust, compact and flexible polymer-based electrodes with high volumetric capacitances.

Conclusions

In conclusion, we have demonstrated an efficient and novel strategy for the fabrication of robust, highly flexible and compact freestanding and binder-free paper electrodes based on nanocellulose fibre reinforced PPy-GO nanocomposites. Since nanocellulose interacts strongly with both the PPy and the GO, its presence reinforces the entire electrode yielding a robust and compact electrode which still contains a sufficient number of mesopores to allow the material to undergo fast PPy charge and discharge reactions. When employed in an aqueous symmetric charge storage device, the PNG paper electrode exhibited the highest volumetric capacitance (i.e. 198 F cm^{-3} based on whole electrode) reported so far for a flexible polymer-based electrode. The robust PNG electrode also exhibited excellent long-term stability with >85 % capacitance retention over 16 000 cycles at 5 A g^{-1}, as well as high volumetric energy and power densities (i.e. 3.4 Wh L^{-1} and 1.1 kW L^{-1}, respectively). The new and straightforward procedures for the fabrication of flexible and dense conducting polymer - based paper electrode described in the present work can readily be employed to manufacture flexible and compact energy storage devices.

Acknowledgements

The Swedish Foundation for Strategic Research (SSF) (grant RMA-110012), The Swedish Energy Agency (project SwedGrids), The Carl Trygger Foundation and the European Institute of Innovation and Technology under the KIC InnoEnergy NewMat and electrical energy storage project, are gratefully acknowledged for financial support of this work.

Notes and references

[a] *Department of Chemistry-The Ångström Laboratory, Uppsala University, Box 538, SE-751 21 Uppsala, Sweden, E-mail: zhaohui.wang@kemi.uu.se;*
[b] *Nanotechnology and Functional Materials, Department of Engineering Sciences, The Ångström Laboratory, Uppsala University, Box 534, SE-751 21 Uppsala, Sweden*

† Electronic Supplementary Information (ESI) available: [details of any supplementary information available should be included here]. See DOI: 10.1039/b000000x/

1. L. Nyholm, G. Nyström, A. Mihranyan and M. Strømme, *Adv. Mater.*, 2011, **23**, 3751-3769.
2. X. Peng, L. Peng, C. Wu and Y. Xie, *Chem. Soc. Rev.*, 2014, **43**, 3303-3323.
3. L. Yuan, X. Xiao, T. Ding, J. Zhong, X. Zhang, Y. Shen, B. Hu, Y. Huang, J. Zhou and Z. L. Wang, *Angew. Chem.*, 2012, **124**, 5018-5022.
4. L. Hu, H. Wu, F. La Mantia, Y. Yang and Y. Cui, *ACS nano*, 2010, **4**, 5843-5848.
5. G. Zhou, F. Li and H.-M. h. Cheng, *Energy Environ. Sci.*, 2013, **7**, 1307.
6. P. Novák, K. Müller, K. Santhanam and O. Haas, *Chem. Rev.*, 1997, **97**, 207-282.
7. H. K. Song and G. T. R. Palmore, *Adv. Mater.*, 2006, **18**, 1764-1768.
8. G. Nystrom, A. Razaq, M. Stromme, L. Nyholm and A. Mihranyan, *Nano Lett.*, 2009, **9**, 3635-3639.
9. G. A. Snook, P. Kao and A. S. Best, *J. Power Sources*, 2011, **196**, 1-12.
10. S. Ghosh and O. Inganas, *Adv. Mater.*, 1999, **11**, 1214-1218.
11. B. Yue, C. Wang, X. Ding and G. G. Wallace, *Electrochim. Acta*, 2013, **113**, 17-22.
12. Z. Niu, P. Luan, Q. Shao, H. Dong, J. Li, J. Chen, D. Zhao, L. Cai, W. Zhou, X. Chen and S. Xie, *Energy Environ. Sci.*, 2012, **5**, 8726-8733.
13. Y. Meng, K. Wang, Y. Zhang and Z. Wei, *Adv. Mater.*, 2013, **25**, 6985-6990.
14. L. Huang, C. Li and G. Shi, *J. Mater. Chem. A*, 2014, **2**, 968-974.
15. M. Kim, C. Lee and J. Jang, *Adv. Funct. Mater.,* 2014, **24**, 2489-2499.
16. X. Lu, H. Dou, C. Yuan, S. Yang, L. Hao, F. Zhang, L. Shen, L. Zhang and X. Zhang, *J, Power Sources*, 2012, **197**, 319-324.
17. H.-P. Cong, X.-C. Ren, P. Wang and S.-H. Yu, *Energy Environ. Sci.*, 2013, **6**, 1185.

18. D.-W. Wang, F. Li, J. Zhao, W. Ren, Z.-G. Chen, J. Tan, Z.-S. Wu, I. Gentle, G. Q. Lu and H.-M. Cheng, *ACS Nano*, 2009, **3**, 1745-1752.
19. J. Benson, I. Kovalenko, S. Boukhalfa, D. Lashmore, M. Sanghadasa and G. Yushin, *Adv. Mater.*, 2013, **25**, 6625-6632.
20. Y. Wang, X. Yang, L. Qiu and D. Li, *Energy Environ. Sci.*, 2013, **6**, 477.
21. Y. Zhou, N. Lachman, M. Ghaffari, H. Xu, D. Bhattacharyya, P. Fattahi, M. R. Abidian, S. Wu, K. Gleason, B. Wardle and Q. Zhang, *J. Mater. Chem. A*, 2014.
22. Q. Wu, Y. Xu, Z. Yao, A. Liu and G. Shi, *ACS Nano*, 2010, **4**, 1963-1970.
23. J. A. Lee, M. K. Shin, S. H. Kim, H. U. Cho, G. M. Spinks, G. G. Wallace, M. D. Lima, X. Lepró, M. E. Kozlov, R. H. Baughman and S. J. Kim, *Nat. Commun.*, 2013, **4**, 1970.
24. M. Paakko, J. Vapaavuori, R. Silvennoinen, H. Kosonen, M. Ankerfors, T. Lindstrom, L. A. Berglund and O. Ikkala, *Soft Matter*, 2008, **4**, 2492-2499.
25. L. Hu, G. Zheng, J. Yao, N. Liu, B. Weil, M. Eskilsson, E. Karabulut, Z. Ruan, S. Fan, J. T. Bloking, M. D. McGehee, L. Wågberg and Y. Cui, *Energy Environ. Sci.* 2013, **6**, 513.
26. L. Jabbour, R. Bongiovanni, D. Chaussy, C. Gerbaldi and D. Beneventi, *Cellulose*, 2013, **20**, 1523-1545.
27. Z. Weng, Y. Su, D.-W. Wang, F. Li, J. Du and H.-M. Cheng, *Adv. Energy Mater.*, 2011, **1**, 917-922.
28. J. M. Malho, P. Laaksonen, A. Walther, O. Ikkala and M. B. Linder, *Biomacromolecules*, 2012, **13**, 1093-1099.
29. N. D. Luong, N. Pahimanolis, U. Hippi, J. T. Korhonen, J. Ruokolainen, L.-S. Johansson, J.-D. Nam and J. Seppala, *J. Mater. Chem.*, 2011, **21**, 13991-13998.
30. L. Yuan, B. Yao, B. Hu, K. Huo, W. Chen and J. Zhou, *Energy Environ. Sci.*, 2013, **6**, 470-476.
31. Z. Wang, P. Tammela, P. Zhang, M. Stromme and L. Nyholm, *J. Mater. Chem. A*, 2014, **2**, 7711-7716.
32. A. Razaq, L. Nyholm, M. Sjödin, M. Strømme and A. Mihranyan, *Adv. Energy Mater.,* 2012, **2**, 445-454.
33. A. Mihranyan, L. Nyholm, A. E. G. Bennett and M. Strømme, *J. Phys. Chem. B*, 2008, **112**, 12249-12255.
34. X. Yang, C. Cheng, Y. Wang, L. Qiu and D. Li, *Science*, 2013, **341**, 534-537.
35. Z. Gui, H. Zhu, E. Gillette, X. Han, G. W. Rubloff, L. Hu and S. B. Lee, *ACS Nano*, 2013, **7**, 6037-6046.
36. A. Davies, P. Audette, B. Farrow, F. Hassan, Z. Chen, J.-Y. Choi and A. Yu, *J. Phys. Chem. C*, 2011, **115**, 17612-17620.
37. Y. Zhao, J. Liu, Y. Hu, H. Cheng, C. Hu, C. Jiang, L. Jiang, A. Cao and L. Qu, *Adv. Mater.*, 2013, **25**, 591-595.
38. V. L. Pushparaj, M. M. Shaijumon, A. Kumar, S. Murugesan, L. Ci, R. Vajtai, R. J. Linhardt, O. Nalamasu and P. M. Ajayan, *Proc. Natl. Acad. Sci. U. S. A.*, 2007, **104**, 13574-13577.
39. K. Gao, Z. Shao, J. Li, X. Wang, X. Peng, W. Wang and F. Wang, *J. Mater. Chem. A*, 2013, **1**, 63.
40. M. M. Hamedi, A. Hajian, A. B. Fall, K. Hakansson, M. Salajkova, F. Lundell, L. Wagberg and L. A. Berglund, *ACS Nano*, 2014, **8**, 2467-2476.
41. K. K. Pandey, *J. App. Poly. Sci.*, 1999, **71**, 1969-1975.
42. Z. Wang, X. Xiong, L. Qie and Y. Huang, *Electrochim. Acta*, 2013, **106**, 320-326.
43. Z. Wang, P. Tammela, P. Zhang, M. Strømme and L. Nyholm, *J. Mater. Chem. A*, 2014, **2**, 16761-16769.
44. Z. Wang, P. Tammela, P. Zhang, J. Huo, F. Ericson, M. Strømme and L. Nyholm, *Nanoscale*, 2014, **DOI:** 10.1039/C4NR04642K
45. A. Burke, *Electrochim. Acta*, 2007, **53**, 1083-1091.
46. J. Zhang, P. Chen, B. H. Oh and M. B. Chan-Park, *Nanoscale*, 2013, **5**, 9860-9866.
47. H. P. de Oliveira, S. A. Sydlik and T. M. Swager, *J. Phys. Chem. C*, 2013, **117**, 10270-10276.
48. H. Fu, Z.-j. Du, W. Zou, H.-q. Li and C. Zhang, *J. Mater. Chem. A*, 2013, **1**, 14943-14950.
49. G. Nyström, M. Strømme, M. Sjödin and L. Nyholm, *Electrochim. Acta*, 2012, **70**, 91-97.
50. D. Zhang, X. Zhang, Y. Chen, P. Yu, C. Wang and Y. Ma, *J. Power Sources*, 2011, **196**, 5990-5996.
51. H. Olsson, G. Nyström, M. Strømme, M. Sjödin and L. Nyholm, *Electrochem. Commun.,* 2011, **13**, 869-871.
52. L. Liu, Z. Niu, L. Zhang, W. Zhou, X. Chen and S. Xie, *Adv, Mater,*, 2014, **26**, 4855-4862.
53. G. Yu, Y. Shi, P. Lijia, B. Liu, Y. Wang, Y. Cui and Z. Bao, *J. Mater. Chem. A*, 2014, **2**, 6086.